Transactions, SMiRT-26
Berlin/Potsdam, Germany, July 10-15, 2022
Division I

INFLUENCE OF HIGH TEMPERATURE HEATING ON THE FRACTURE PROPERTIES OF CONCRETE MIXED WITH DIFFERENT COARSE AGGREGATE

Koichi Matsuzawa[1], Yoshinori Kitsutaka[2]

[1] Senior Research Engineer, Dept. of Building Materials and Components, Building Research Institute, Japan (matsu@kenken.go.jp)
[2] Prof., Dept. of Architecture and Building Engineering, Graduate School of Urban Environmental Sciences, Tokyo Metropolitan University, Dr. Eng.

ABSTRACT

This paper reports on the influence of coarse aggregate types on the fracture properties of concrete subjected to high temperatures up to 800°C. The fracture properties were evaluated based on tension-softening curves determined by polylinear approximation through inverse analysis. And the follow conclusions were found: The initial cohesive stress of concrete containing sandstone, granodiorite, and chert slightly increased, while those of limestone slightly decreased at 100°C, and at higher temperatures, the initial cohesive stress of all specimens decreased. The fracture energy of all specimens increased up to a heating temperature of 300°C but then tended to decrease.

INTRODUCTION

With the broadening of their uses, concrete structures are subjected to a wide variety of deteriorative factors during their working life. Heat is one such factor, which alters the strength properties of concrete. For this reason, temperature limits may be set on concrete in service for structures subjected to heat for a long time, such as power generation facilities. The properties of concrete also change in a fire due to high temperature heating. Active investigation has therefore been carried out on concrete affected by heat. It has been reported that compressive strength is changed by increasing heat and the concomitant moisture state, decreasing to a greater extent as the temperature rises. Tensile strength is also reported to decrease with the heating temperature, with the loss being greater than the loss in compressive strength. These changes, which vary depending on the presence/absence and type of aggregate, have been summarized in reports by NRC (2010) and AIJ (2009). Since concrete subjected to high temperature heating can suffer strength loss, it can also be prone to cracking. However, there have been few reports on cracking in concrete under the effect of high temperature heating. Cracking occurs primarily due to fracture in tension. The evaluation of fracture propagation due to tensile deformation is therefore necessary for investigating the occurrence and propagation of cracking. To this end, it is considered effective to indirectly determine the tension softening curve by applying fracture toughness testing, which provides a stable load-displacement relationship including the softening phase after the maximum load of concrete under tensile deformation.

The authors (2013, 2015) have investigated high temperature heating in relation to the fracture parameters obtained from fracture toughness testing. In the present study, the authors fabricated concrete specimens containing different types of coarse aggregates and mortar specimens with no coarse aggregate, exposed these specimens to high temperatures ranging from 100 to 800°C for 168 h, and conducted wedge splitting tests. Fracture parameters were then calculated based on inverse analysis of the tension softening curves of these specimens. The effect of coarse aggregate types on the fracture properties of concrete subjected to high temperature heating was investigated based on results.

EVALUATION OF FRACTURE PROPERTIES

Method of estimating tension softening curve

Fracture properties were evaluated based on tension-softening curves, which were determined by polylinear approximation through inverse analysis of load versus crack mouth opening displacement (CMOD) curves obtained from wedge splitting tests using an analysis program devised by the authors (1994, 1997, 2001). Specifically, evaluation was carried out using initial cohesive stress and fracture energy obtained from tension-softening curves.

The tension-softening curve is an index expressing the relationship between the cohesive force and CMOD where the fracture propagation is simulated by a cohesive force model. The initial cohesive stress on the curve serves as a parameter representing the intrinsic tensile strength of the material. Initial cohesive stress expresses the crack initiation resistance. The larger this value, the greater the resistance to crack initiation.

The area enclosed with a tension-softening curve represents the fracture energy necessary for making the width between the nodes of a fictitious crack opening to reach the limit opening displacement for complete separation. Fracture energy expresses the crack propagation resistance. The larger this value, the greater the resistance to crack propagation.

EXPERIMENT OVERVIEW

Outline of specimens

Table 1 gives the materials. Four rock types generally used for concrete were used for coarse aggregate. Figure 1 shows the X-ray powder diffraction data of the aggregates. This was measured using an X-ray powder diffractometer manufactured by Bruker AXS, with the X-ray source, tube voltage, tube current, scan range, and step width being Cu-Kα, 30 kV, 10 mA, 2 θ = 5 to 65°, and 0.02°, respectively. The minerals listed in Table 1 are major minerals detected in the rocks by X-ray diffraction. Quartz is found to be present in sandstone, granodiorite, chert, and land sand, and calcite is found in limestone. Tables 2 and 3 give the mixture proportions and test factors/levels, respectively. Four different types of rock were used as coarse aggregate. Concrete was proportioned with a water-cement ratio, target slump, and target air content of 57%, 18 cm, and 4.5%, respectively. The coarse aggregate content was kept constant at 356 litters/m^3, while the slump and air content were adjusted by the admixture dosage.

Table 1: Materials

Materials	Mark	Details
Cement	C	Ordinary Portland cement, Gravity=3.16g/cm^3
Fine aggregate	S	Land sand, Specific gravity=2.58 g/cm^3, F.M.=2.68 Mineral composition: Quartz (SiO_2), Albite ($NaAlSi_3O_8$), Muscovite ($KAl_2(AlSi_3)O_{10}(OH)_2$)
Coarse aggregate	G1	Sandstone, Specific gravity=2.66 g/cm^3, Absolute volume=62.4% Mineral composition: Quartz (SiO_2), Anorthite ($CaAl_2Si2O_8$), Albite ($NaAlSi_3O_8$), Muscovite ($KAl_2(AlSi_3)O_{10}(OH)_2$)
	G2	Granodiorite, Specific gravity=2.71 g/cm^3, Absolute volume=59.5% Mineral composition: Anorthite ($CaAl_2Si2O_8$), Albite ($NaAlSi_3O_8$), Quartz (SiO_2), Clinochlore ($(Mg,Fe)_5Al(Si_3Al)O_{10}(OH)_8$), Magnesiohornblende ($Ca_2Mg_4AlSi_7AlO_{22}(OH)_2$)
	G3	Limestone, Specific gravity=2.71 g/cm^3, Absolute volume=61.0% Mineral composition: Calcite ($CaCO_3$)
	G4	Chert, Specific gravity=2.64 g/cm^3, Absolute volume=58.0% Mineral composition: Quartz (SiO_2), Muscovite ($KAl_2(AlSi_3)O_{10}(OH)_2$)
Admixture	Ad	Air entraining and reducing agent

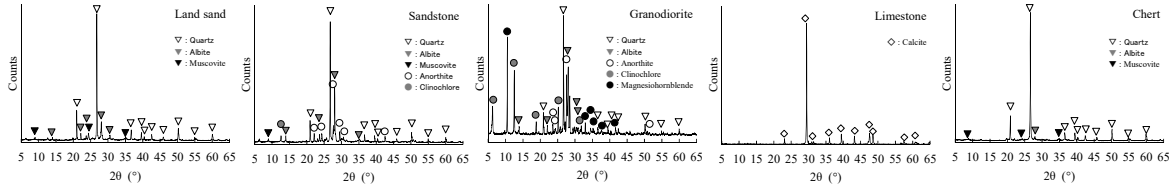

Figure 1. X-ray diffraction spectrum of aggregates

Table 2: Factors and levels

Factors	Levels
Specimens	Concrete, Mortar
Coarse aggregate	Sandstone, Granodiorite, Limestone, Chert
Maximum temperature (°C)	100, 200, 300, 400, 500, 600, 700, 800

Table 3: Mixture proportions (in kg/m^3)

Coarse aggregate	W/C (%)	W	C	S	G1	G2	G3	G4	Ad
Sandstone	57.0	175	307	844	947	-	-	-	2.46
Granodiorite	57.0	175	307	844	-	965	-	-	4.30
Limestone	57.0	175	307	844	-	-	965	-	2.46
Chert	57.0	175	307	844	-	-	-	940	4.61
- (Mortar)	57.0	292	512	1409	-	-	-	-	-

A pan-type mixer with a capacity of 100 litters was used for mixing. The concrete mixing procedure was as follows: Place cement and fine aggregate in the mixer and mix for 10 sec; add water and the chemical admixture and mix for 30 sec; then add coarse aggregate and mix for 90 sec. The mixing procedure for mortar was as follows: Place cement and fine aggregate in the mixer and mix for 10 sec; add water and the chemical admixture and mix for 30 sec; scrape off the materials from the mixer wall back into the batch and mix for 90 sec. The batch size was 100 litters. Three batches were mixed for each mixture design. The concrete and mortar were placed in molds after fresh testing.

Three specimens for wedge splitting tests to evaluate the fracture properties, 100 × 100 × 120 mm in size, were fabricated for each set of conditions. The number of cylinders for measuring the compressive strength and elastic modulus, 100 mm in diameter and 200 mm in height, was also three for each set of conditions. These specimens were demolded 2 days after placing, water-cured at 20°C up to an age of 26 weeks, and then subjected to heating followed by testing. Table 4 gives the fresh properties and strength test results at the ages of 4 and 26 weeks.

Table 4: Properties of concrete

Coarse aggregate	Slump (cm)	Air (%)	Compressive strength (N/mm^2)		Young's modulus (kN/mm^2)	
			4 weeks	26 weeks	4 weeks	26 weeks
Sandstone	17.5	4.3	39.3	45.5	27.9	31.7
Granodiorite	18.0	4.2	40.1	46.5	25.7	28.9
Limestone	17.5	4.4	39.0	47.3	31.1	33.1
Chert	17.5	5.1	38.2	43.5	27.7	30.3
- (Mortar)	-	-	46.0	57.0	24.0	27.1

Test procedures

Figure 2 shows the temperature histries in the furnace, with the maximum temperature in the furnace while heating specimens being 100, 200, 300, 400, 500, 600, 700, and 800°C. Tests were also conducted on unheated (20°C) specimens for comparison. Two programmable muffle furnaces (inside W310 × D610 × H310 mm) with heaters on both side walls were used for heating. To achieve uniform heating, specimens were placed in the center so as to equalize the distances from both heaters. A temperature rise rate of 0.5°C/min was adopted to minimize the difference between the temperatures on the surface and in the center of each specimen. When the heating phase was completed, specimens were allowed to cool naturally to the level of outdoor air temperature and subjected to testing.

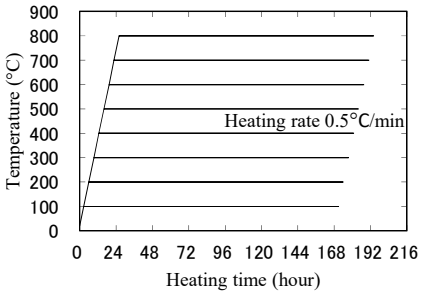

Figure 2. Temperature histories

The thermal expansion of the four types of rocks used as coarse aggregate and matrix mortar was measured using a thermomechanical analyzer manufactured by NETZSCH JAPAN. Pieces of the mortar and four types of rocks approximately 7 × 7 × 17-20 mm in size were prepared as test pieces. Rock pieces in the air-dry condition and mortar in the saturated surface dry condition were heated from room temperature up to 1,000°C at a temperature rise rate of 5°C/min with a N_2 flow of 200 ml/min to measure their expansion. Note that measurement began after keeping the temperature in the furnace containing the test pieces at 30°C for 1 h.

RILEM. (1994) and Japan Concrete Institute. (2003) specify three-point flexure tests on notched beams, to induce mode I failure (tensile), as a method of evaluating the fracture toughness of concrete. However, this method requires large specimens with a typical size of 100 × 100 × 400 mm. When evaluating the fracture properties of concrete using such specimens, the effect of their own weight cannot be ignored. The effect of specimens' own weight is expected to be particularly significant when dealing with concrete affected by high temperature heating as in this study. This is because concrete becomes brittler after heating, making the effect of the weight of specimens on their fracture properties relatively stronger than testing at normal temperatures. It was therefore considered that small specimens would lead to smaller errors in test values. Also, minimizing the specimen size is more advantageous from the aspect of uniform heating in the furnace. For these reasons, wedge splitting testing was adopted in this study, as it provides mode I failure, similarly to three-point loading on notched beams, for small-sized 100 × 100 × 120 mm (Figure 3).

A notch was cut in the center of one side of each specimen for wedge splitting testing before heating to leave a ligament depth of 50 mm using a diamond cutter with a blade thickness of 1 mm, in order to induce tensile failure by inserting a wedge into the notch. The size of jigs used for the test conformed to the test method proposed by RILEM (1994). Since concrete affected by high temperature heating becomes brittler, its resistance to tensile forces can be significantly reduced. It is therefore necessary to accurately detect the post-peak softening zone for measuring a stable load-CMOD curve. To this end, a servohydraulic testing machine of a closed-loop system type was used. This is a machine manufactured by MTS Systems Corporation, comprising the loading unit, hydraulic unit, and control unit having a feedback function. Also, the rate of CMOD at the opening mouth was set at 0.02 mm/min so as to lead to stable failure of each specimen. Note that sensitive clip gauges for controlling displacement were used for measuring the CMOD.

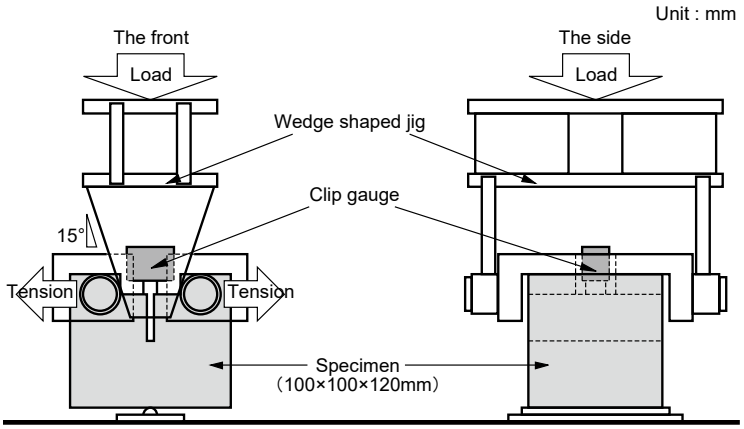

Fig. 3. Wedge splitting test

RESULTS AND DISCUSSION

Thermal expansion properties

Figure 4 shows the thermal expansion-temperature relationship. All rocks used for coarse aggregate expand as the temperature rises. The expansion of sandstone, granodiorite, and chert is up to 550°C but becomes rapid in the range of 550 to 600°C. That of mortar containing land sand as fine aggregate is not appreciable up to around 550°C but becomes rapid in the range of 550 to 600°C similarly to sandstone, granodiorite, and chert. It should be noted that limestone expands with temperature but begins to shrink at 890°C.

Sandstone, granodiorite, chert, and land sand contain quartz, which rapidly expands at 575°C when it undergoes phase transition from α to β. This is presumably the reason for the expansion of sandstone, granodiorite, and chert, as well as mortar containing land sand. The shrinkage of limestone can be attributed to the release of CO_2 from calcite, its principal mineral, due to its thermal decomposition in the range of 650 to 900°C.

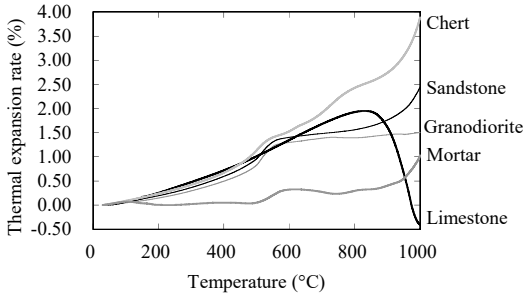

Fig. 4. Thermal expansion rate-temperature relationship

Mass change

Figure 5 shows the mass change-heating temperature relationship. The mass change ratio of mortar is greater than those of concretes, presumably due to the unit water content of mortar being greater than that of concrete. No marked difference is observed between coarse aggregate types of concretes. The mass loss ratios of both mortar and concrete specimens are greater up to 100°C than thereafter, primarily due to the escape of free water. The mass of all specimens decreases nearly linearly in the range higher than 100°C.

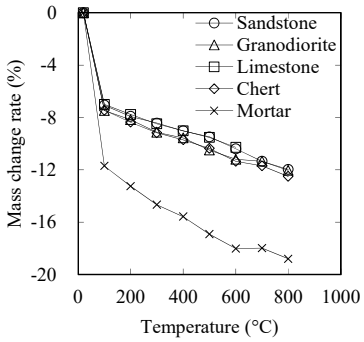

Fig. 5. Mass change-heating temperature relationship

Mechanical properties

Figures 6 and 7 show the compressive strength and the residual compressive strength (RCS) ratio to 20°C, respectively, related to the heating temperature. The compressive strength of mortar is greater than those of concretes. While the strengths of concretes containing sandstone (CS), granodiorite (CG), and chert (CC) are nearly the same, that of concrete containing limestone (CL) is slightly lower. This is presumably because more cracks and voids are generated at the boundaries between mortar and limestone aggregate than in other specimens during the cooling phase, in which limestone undergoes a greater shrinkage. It should be noted that, at heating temperatures of 100°C or higher, the compressive strengths of all specimens decrease at similar rates regardless of the presence/absence and type of coarse aggregate. This is presumably because bonding water is lost due to thermal decomposition of C-S-H at 100 to 300°C and $Ca(OH)_2$ at 400 to 500°C, resulting in embrittlement of mortar.

At 100°C, the RCS ratios of CS, CG, CL, CC, and mortar containing no coarse aggregate are 0.97, 1.01, 0.86, 1.03, and 1.07, respectively. This means that the compressive strength of mortar increases, that of CS, CG, and CC scarcely changes, and that of CL decreases up to 100°C. This can be explained as follows: The temperature rise accelerated the hydration of unhydrated cement in mortar, densifying the microstructure of mortar to increase its compressive strength. In the case of concrete, however, the difference between the expansion coefficients of mortar and coarse aggregate causes a difference in their strains, generating microcracks. The strength of concrete therefore decreases or scarcely changes. The RCS ratio of CL after heating tends to be smaller than those of CS, CG, and CC.

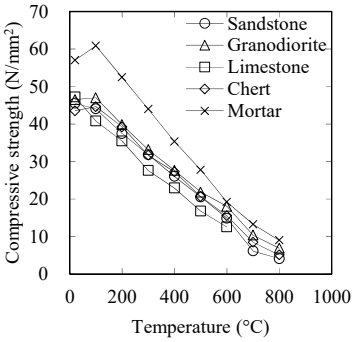

Fig.6. Compressive strength -heating temperature relationship

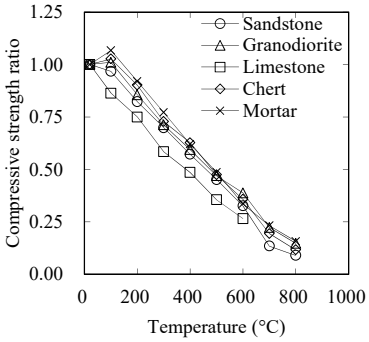

Fig.7. Residual compressive strength ratio -heating temperature relationship

Figures 8 and 9 show the Young's modulus and residual Young's modulus (RYM) ratio, respectively, related to the heating temperature. Before heating, the Young's modulus of mortar is lower than that of concrete, but both decrease in a similar manner as the heating temperature rises. Also, the Young's modulus of CL tends to be smaller than that of concretes containing other aggregates.

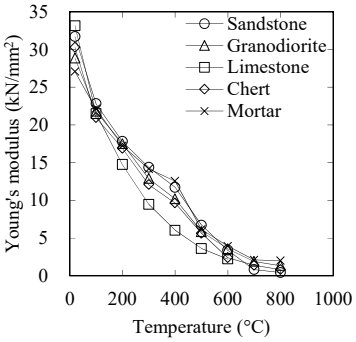

Fig.8. Young's modulus -heating temperature relationship

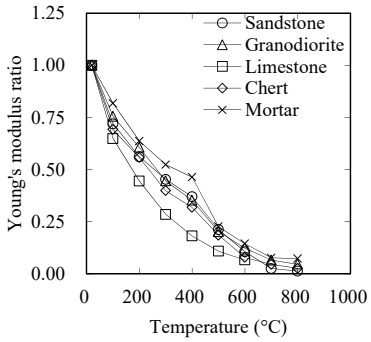

Fig.9. Residual Young's modulus ratio -heating temperature relationship

Load-Crack mouth opening displacement (L-CMOD) curve

Figure 10 shows the L-CMOD curves of specimens. The maximum loads on the L-CMOD curves of LS are similar up to 300°C, the maximum load of other specimens at 100°C is higher than that at 20°C. When comparing the maximum loads at each temperature, that of mortar is the highest and that of CL is the lowest. Presumably, the former is due to the high content of paste, and the latter is due to the large shrinkage of limestone after heating, which cause voids and cracks in the mortar-limestone interfaces during cooling. CS, CG, and CC show similar tendencies of L-CMOD curves presumably due to their similar tendencies of thermal expansion properties during heating (Fig. 4).

As to the shapes of the curves, the gradient of the increasing load with the increase in the CMOD is steep and linear, followed by rapid post-peak reduction, while the heating temperature is low, regardless of the coarse aggregate type. As the heating temperature increases, however, the gradient of the increasing load becomes less steep, followed by slow post-peak reduction. This can be explained as follows: Cracking under loading propagates linearly while the heating temperature is low, as no such defects as microcracks are present in the fracture process zone (FPZ), leading to brittle fracture. When the heating temperature is high, cracking propagates through the FPZ where many defects including microcracks are present. Therefore, fracture does not become brittle, with reduction in the load being gentle.

Tension softening curve

Figure 11 shows the tension-softening curves of specimens. The decreasing tendencies of cohesive stress with the increase in the CMOD vary depending on the presence/absence and type of coarse aggregate. The initial cohesive stress of mortar is higher than those of concretes, with the reduction in the cohesive stress associated with the increase in the CMOD being slower. Whereas the tendencies of CS, CG, and CC are similar, the cohesive stress loss of CL with the increase in the CMOD is slightly greater than the others.

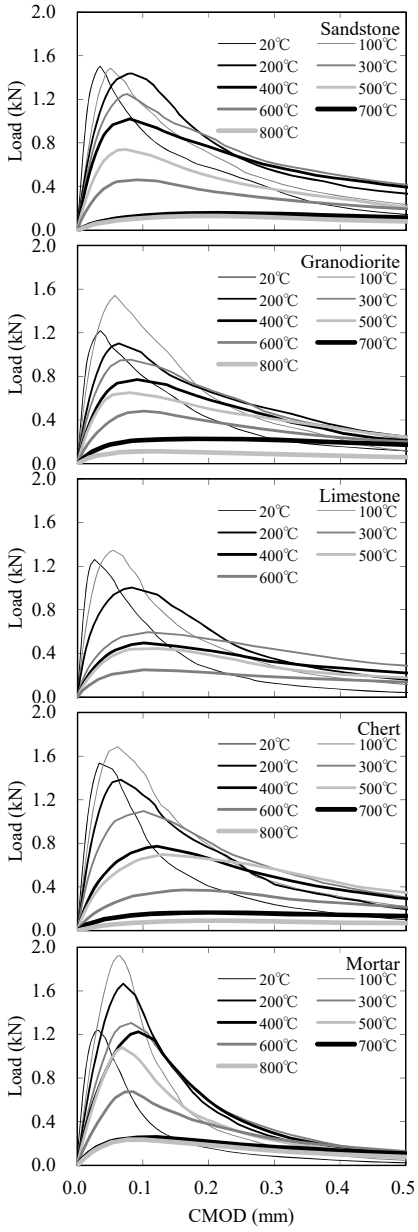

Fig. 10. L-CMOD curve

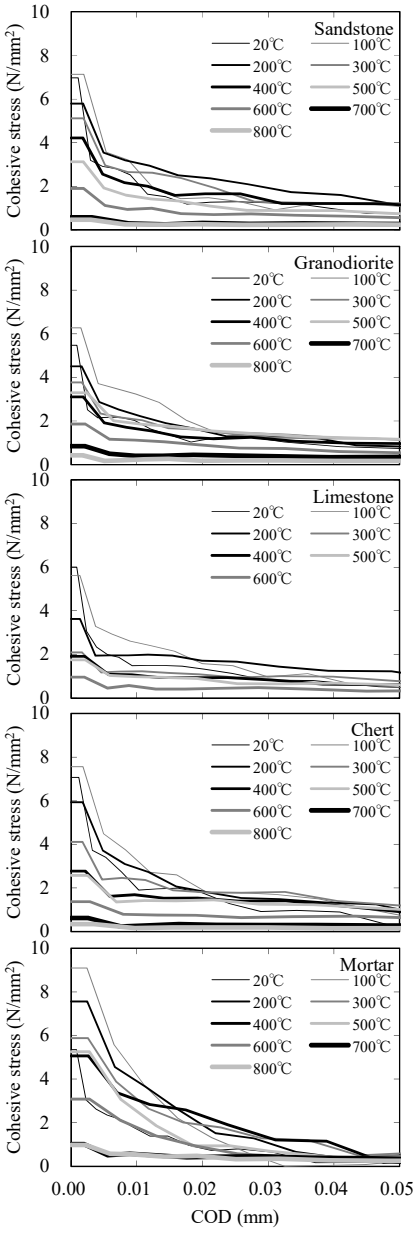

Fig. 11. Tension-softening curve

Fracture properties

Figures 12 and 13 show the initial cohesive stress and residual cohesive stress ratio with respect to the value at 20°C, respectively, related to the heating temperature. The initial cohesive stress of CS and CC before heating is around 7 N/mm^2, while that of CG, CL, and mortar is around 6 N/mm^2. After heating, the cohesive stress of mortar with a high content of cement paste, the binder, significantly increases, while that of CS, CG, and CC slightly increases, and that of CL decreases. The slight increase in the cohesive stress of CS, CG, and CC at 100°C is presumably due to hydration of unhydrated cement being accelerated by heating.

The reduction in the cohesive stress of CL at 100°C is presumably due to the large shrinkage of limestone after heating, which causes a large number of voids and cracks at mortar interfaces. At heating temperatures of over 100°C, the cohesive stress of all specimens decreases as the heating temperature increases. This can be attributed to the modification and loss of cement hydrates due to dehydration of bonding water resulting from thermal decomposition of C-S-H and $Ca(OH)_2$, as well as to the conflicting expansion-shrinkage behavior of shrinking cement paste and expanding aggregate.

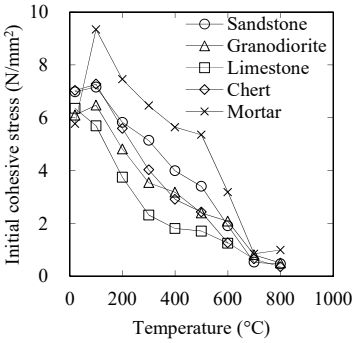

Fig.12. Initial cohesive stress -heating temperature relationship

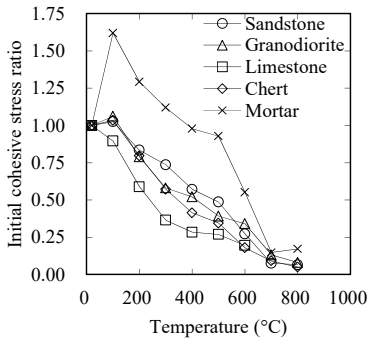

Fig.13. Initial cohesive stress ratio -heating temperature relationship

Figures 14 and 15 show the fracture energy and residual fracture energy ratio, respectively, related to the heating temperature. The fracture energy of CS, CC, CG, CL, and mortar before heating is 130, 110, 100, 80, and 60 N/m, respectively. After heating, the fracture energy of all specimens tends to increase with the heating temperature up to 300°C and decrease thereafter. This can be explained as follows: Up to around 300°C, cohesive stress increases due to accelerated hydration of unhydrated cement, and thermal decomposition of C-S-H and $Ca(OH)_2$ dehydrates cement hydrates by removing binding water to cause their modification and disappearance. Conflicting expansion-shrinkage behavior is also brought about by shrinking cement paste and expanding aggregate. These phenomena cause microcracks, expanding the FPZ. Fracture under loading therefore propagates through the zone in a branching manner, increasing further cracks during propagation, thereby increasing the energy required for fracture. The fracture energy thus increases up to the heating temperature of 300°C. At higher temperatures, however, the effects of the modification and loss of cement hydrates become greater to further expand the FPZ, but the cohesive stress decreases. Thus the energy required for fracture propagation decreases, leading to lower fracture energy.

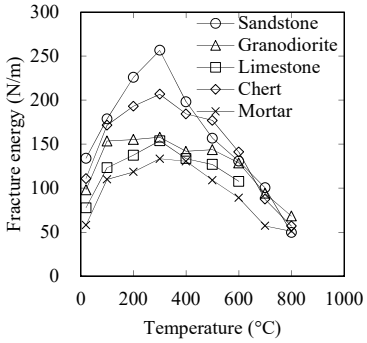

Fig.14. Initial cohesive stress -heating temperature relationship

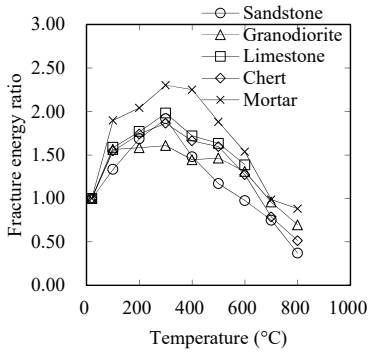

Fig.15. Residual Initial cohesive stress ratio -heating temperature relationship

CONCLUSION

In this study, the effect of coarse aggregate types on the fracture properties of concrete subjected to high temperature heating from 100 to 800°C for 168 h was investigated. As a result, the following were found within the range of this study:

(1) The fracture surface areas of both concrete and mortar affected by high temperature heating linearly increase as the temperature rises. The fracture surfaces of concrete tend to be larger than those of mortar.
(2) The maximum load of sandstone on the L-CMOD curve scarcely changes up to 300°C, whereas those of other specimens are highest at 100°C. When comparing the maximum loads at the same heating temperatures, that of mortar is higher and that of limestone is lower than the others.
(3) The tension softening curves express generally decreasing cohesive stress with the increase in the COD. Amid these trends, the cohesive stress of mortar, whose initial cohesive stress is greater than those of concretes, decreases at a slower rate than those of concretes. As to concrete specimens, the reductions in the cohesive stress of sandstone, granodiorite, and chert take on similar trends, but that of limestone is slightly faster than the other concrete specimens.
(4) At a heating temperature of 100°C, the initial cohesive stress of mortar significantly increases, while those of sandstone, granodiorite, and chert slightly increase and that of limestone slightly decreases. At higher temperatures, the initial cohesive stress decrease.
(5) Up to a heating temperature of 300°C, the fracture energy of all specimens increase but then tends to decrease as the heating temperature increases.

REFERENCES

NRC Job Code N6511. (2010). "A Compilation of Elevated Temperature Concrete Material Property Data and Information for Use in Assessments of Nuclear Power Plant Reinforced Concrete Structures." U.S.NRC.

Architectural Institute of Japan. (2009). "Guide Book for Fire-Resistive Performance of Structural Materials."

Matsuzawa K. and Kitsutaka Y. (2013). "Evaluation on the fracture properties of concrete subjected to high temperature heating." *Transactions*, SMiRT22, 10p, USB.

Matsuzawa K. and Kitsutaka Y. (2015). "Influence of heating time on fracture properties of concrete." *Transactions*, SMiRT23, 9p, USB.

Kitsutaka Y., Kamimura K., and Nakamura S. (1994). "Evaluation of aggregate properties on tension softening behavior of high strength concrete, High Performance Concrete," *American Concrete Institute*, ACI SP 149-40, 711-727.

Kitsutaka Y. (1997). "Fracture parameters by polylinear tension-softening analysis," *J. Engrg. Mech.*, ASCE., Vol. 123:5., 444-450.

Kitsutaka Y. and Takahashi, Y. (2001). "Fracture mechanics based bending failure analysis for fiber reinforced light-weight concrete panel considering crack dispersion effect," *J. Struct. Constr. Eng.*, AIJ, No.541, 37-42. (in Japanese)

RILEM AAC13.1. (1994). "Determination of the specific fracture energy and strain softening of AAC." *RILEM Recommendations for the Testing and Use of Constructions Materials*, 156-158.

JCI-S-001-2003. (2003). "Method of test for fracture energy of concrete by use of notched beam"